Hindawi Publishing Corporation
Advances in Meteorology
Volume 2009, Article ID 105265, 9 pages
doi:10.1155/2009/105265

Research Article

Comparisons of the Generalized Potential Temperature in Moist Atmosphere with the Equivalent Potential Temperature in Saturated Moist Atmosphere

Yushu Zhou,[1] Liping Liu,[2] and Guo Deng[3]

[1] *Laboratory of Cloud-Precipitation Physics and Severe Storms (LACS), Institute of Atmospheric Physics, Chinese Academy of Sciences, Beijing 100029, China*
[2] *State Key Laboratory of Severe Weather, Chinese Academy of Meteorological Sciences, Beijing 100081, China*
[3] *National Meteorological Center, China Meteorological Administration, Beijing 100081, China*

Correspondence should be addressed to Yushu Zhou, zys@mail.iap.ac.cn

Received 13 November 2008; Accepted 3 March 2009

Recommended by Shouting Gao

The real tropospheric atmosphere is neither absolutely dry nor completely saturated. It is in general moist but not saturated. Here the generalized potential temperature (GPT) was introduced to describe this humid feature of real moist atmosphere. GPT's conservation property in moist adiabatic process was discussed and proved. Comparisons of GPT in moist atmosphere with the equivalent potential temperature (EPT) in saturated moist atmosphere were made by analyzing three torrential rain cases occurring over Jianghuai Valleys in 2003, the north China in 2004, and with the typhoon Fung-Wong in 2008, respectively. Results showed that the relative humidity is not up to 100% even in torrential rain systems, the saturated condition for EPT is not always held, and thus GPT can describe the moisture concentration and moisture gradient better than EPT. The GPT's definition includes the process that the air changes from dry to moist, then up to saturated. Therefore, potential temperature (PT) and EPT can be considered as its two special status. Similar as PT and EPT, GPT can be used to study atmospheric dynamic and thermodynamic processes more generally because of its conservation property in moist adiabatic process.

1. Introduction

Potential temperature (abbreviated as PT and denoted by θ) is an important parameter for dry atmosphere and can be used for comparing the thermodynamic discrepancy of air parcels under different pressure. However if latent heat release is involved, θ is not conservative. So the equivalent potential temperature (abbreviated as EPT and denoted by θ_e), conserved in the saturated and moist adiabatic expansion, is introduced to describe saturated atmosphere [1]. For its conservation property, θ_e has been widely used in many studies of moist atmospheric processes, such as the analysis of stability [2], the extratropical cyclone [3] as well as the investigation of squall line [4], frontal surface, and rainbands [5, 6]. Although widely applied, both PT and EPT have their own scopes of application: PT is suitable for absolutely dry air and EPT in general for the absolutely saturated, moist air only. But the real atmosphere is neither totally dry nor completely saturated. It is moist but unsaturated. Gao et al. [7] defined the atmospheric state that the air is saturated somewhere but not everywhere as the nonuniform saturation. To avoid confusing the two air states, here the moist atmosphere is defined as the moist but unsaturated air, which is more similar to the real one. So the conservation of PT and EPT may not properly be applied to the moist atmosphere.

Other than the absolutely dry or completely saturated air, the moist atmosphere is the real object of atmospheric research. Because the phase changes and microphysical processes are hard to observe and estimate, progress in these fields is very slow. Xie [8] advocated the work of the moist atmospheric dynamics in 1970s. Since then many Chinese scholars pursued in this area [9–11] but the works are still relatively insufficient. In other countries,

investigations about the dynamics of moist air have been carried out. For example, Tripoli and Cotton [12] argued that PT for the mixture of ice-water θ_{il} has a big advantage over θ in identifying atmospheric deep convective systems; Pointin [13] emphasized the thermodynamic impacts of precipitation and defined the moist equivalent temperature (θ_q) substituting T and PT in modeling calculations; in the perspective of entropy, Hauf and Höller [14] considered that the different forms of PT could be expressed by a universal physical variable, namely, the entropic temperature θ_s. By introducing the concept of virtual temperature T_ρ into thermodynamic process on the basis of ice phase interaction, Ooyama [15, 16] derived a set of direct, consistent criteria of dynamics and thermodynamics, which are connected with the parameterization of physical processes. In order to analyze the potential impacts of the change of potential vorticity with the help of ice crystal, Rivas Soriano and García Díez [17] derived a tendency equation for the generalized potential vorticity q_g with the help of θ_s and drew a conclusion that inhomogeneous heating is associated with the development of connective system. Under the nonstatic, moist, and rainy atmosphere, Schubert et al. [18], utilizing the physical quantity θ_ρ proposed by Ooyama [15], discussed the new potential vorticity theory. Not using the approach of parameterization of physical processes, Bannon [19] provided a set of moist air equations to predict the short- or long-term weather by means of integrating the original dynamic equations. The works mentioned above in addition to Betts [20] and Persson [21] applied a large number of variables and empirical constants for describing the properties of the real atmosphere in which dry air, water vapor, and hydrometeors (liquid water) coexist. However, these various approaches resulted in implicit physical meanings of new variables and complicated calculations, and thus are inconvenient for practical analyses, thereby not widely used in operations.

Gao et al. [7] introduced a parameter, called the generalized potential temperature and denoted as θ^*, into the atmospheric framework, which is connected with specific humidity reflecting the traits of the actual atmosphere—neither absolutely dry nor totally saturated. By adding two variables, namely, specific humidity and saturation specific humidity, which are already in the expression of EPT, into the formula of θ^*, the easily calculated and novel parameter θ^* is proposed, having shown great potential in the real weather analyses. Furthermore, with the help of θ^*, a series of analysis and prediction approaches have been tested, including analyzing and identifying heat wave weathers during the summer season of Beijing [22], and diagnosing rainstorms in the nonuniformly saturated flow by adopting the ageostrophic Q vector [23]. However these works have not directly touched whether and how GPT may physically conserve. Suppose GPT is conserved in the adiabatic process of real moist atmosphere, just as PT in the dry adiabatic process and EPT in the saturated moist adiabatic process, the basis and scope of application can further be guaranteed. Therefore, this paper focuses on exploring GPT's physical meanings, demonstrating its conservation in moist atmosphere and further comparing its distribution with those for EPT in a variety of torrential rain cases, because the moist atmosphere and precipitation processes are focuses in this paper.

2. The Definition of GPT and Its Conservation Law for Moist Atmosphere

The expression of GPT for the nonuniformly saturated air, introduced by Wang and Luo [9], can be written as $\theta^*(T,p) = \theta(T,p)\exp((Lq_s \cdot (q/q_s)^k)/c_{pm}T)$, here, T is the atmospheric temperature, p is the pressure, θ is the potential temperature (PT) of dry air, q and q_s are the specific humidity and the saturated specific humidity, respectively, L and c_{pm} are the latent heat per unit mass of condensation and the specific heat per unit mass at constant pressure of moist air, and the $(q/q_s)^k$, known as the function of condensation probability, is a reflection of the humidity of the real air. When air is dry ($q = 0$), GPT means PT, namely, $\theta^*(T,p) = \theta(T,p)$; When air is saturated ($q = q_s$), GPT turns into EPT, namely, $\theta^*(T,p) = \theta(T,p)\exp(Lq_s/c_{pm}T) = \theta_e$; when q varies from 0 to q_s, θ^* has a value between θ and θ_e, which can manifest the changes of the air from dry to moist, then up to saturated. PT and EPT are the two extremes of GPT.

2.1. Physical Discussions of the Condensation Probability Function in Moist Atmosphere. On the basis of the molecular statistics, if the specific humidity of the air is q, the specific humidity of an infinitesimal part q' probably does not equal q but follows a certain statistical distribution [24]. According to the observations, due to a large number of condensation nucleuses in the air, some parts of the air condense (usually condensation starts as the relative humidity (RH) reaches 76%) before the relative humidity is near 100%. Commonly, the higher the value of RH is, the easier the vapor condenses, which means the degree of condensation of vapor increases with the increasing humidity. In order to apply this microphysical property of moist air to weather analyses, it is reasonable to add a weighted function y into EPT without changing its dimension, so a new parameter is derived as the form of $\theta^* = \theta\exp((L/C_pT)q_sy)$. This weighted function y, indicating the coexistent feature of dry and moist air, should satisfy the following conditions: $y = 0$ in absolute dry air and $y = 1$ in totally saturated moist air. Hence, based on the facts that the condensation increases with the increasing humidity, y must be a dimensionless parameter but is associated with humidity. In order to apply this theory into the synoptic system diagnosis and approach, the form of power function $y = (q/q_s)^k$ is adopted in our study. According to the numerical simulation and data analysis [24], the condensation feature can be perfectly described when k is settled by 9. Obviously, there are many other forms of y in addition to $y = (q/q_s)^k$.

The real atmosphere is neither absolutely dry nor completely saturated, therefore it is rational to introduce the condensation probability function and further study the dynamic and thermodynamic processes of the moist air.

2.2. The Conservation of GPT. In view of the small changes of a closed system, the first law of thermodynamics can be expressed by

$$\delta U = \delta Q + \delta W, \tag{1}$$

where δU is the increment of the internal energy for the system, δQ is the heat which the system gains in the process, and δW is the work done to the system. Applying the equation of state, (1) can be written as

$$\delta U = T\delta S - p\delta V. \tag{2}$$

Here, S is the entropy. Another form of (2) is

$$\delta H = T\delta S + V\delta p, \tag{3}$$

where H is the enthalpy of the system. Owing to (2) and (3) involving the state equation, for whatever processes (irreversible or reversible), (1)–(3) can satisfy the conditions. Considering the reversible process, the following equation holds:

$$\delta Q = T\delta S, \qquad \delta W = -p\delta V. \tag{4}$$

As to the ideal gas per unit mass, its internal energy and enthalpy can be expressed by

$$U = c_v T, \tag{5}$$

$$H = c_v T + RT = c_p T. \tag{6}$$

Here, c_v and $c_p = c_v + R$ are the specific heat per unit mass at constant volume and pressure, respectively. Suppose the change of c_v has nothing to do with T.

Equation (6) and $V = 1/\rho = RT/p$ are substituted into (3), thus

$$T\delta S = c_p \delta T - \frac{RT}{p}\delta p. \tag{7}$$

On the both sides of (7) multiplied by $1/T$, we get

$$\delta S = \frac{c_p}{T}\delta T - \frac{R}{p}\delta p = c_p \delta(\ln T) - R\delta(\ln p). \tag{8}$$

When the air parcel becomes saturated, specific humidity q is equal to $q_s(T, p)$. Suppose a vapor parcel is lifted with an increment of δz, the change of saturated specific humidity is $|\delta q_s| = -\delta q_s$. The related latent heat is

$$\delta Q = -L\delta q_s. \tag{9}$$

In this process, liquid water drops out of the air parcel and is not involved in the course of heat balance. Under this assumption, it is a nonadiabatic process. Comparing to the heat still left in the parcel, however the heat taken out by liquid water can be ignored. Thus the process can be considered pseudo-adiabatic [25].

Based on the property of nonuniform saturation, the latent heat release can be expressed as

$$\delta Q = -L\delta(q_s \cdot y). \tag{10}$$

Furthermore, employing the appropriate form of y, it yields

$$\delta Q = -L\delta\left(q_s \cdot \left(\frac{q}{q_s}\right)^k\right). \tag{11}$$

Taking (4) into (8), we get

$$c_{pm}\delta(\ln T) - R_v\delta(\ln p) = \frac{\delta Q}{T} = -\frac{L\delta\left(q_s \cdot (q/q_s)^k\right)}{T}, \tag{12}$$

where c_{pm} is the specific heat of moist air under constant pressure and R_v is the specific gas constant of vapor.

From the curve change of $q_s(T, p)$ based on the long-term observations (not shown; see Zhao and Gao [26]), the inequality $q_s(q/q_s)^k \ll 100\,\mathrm{g}\cdot\mathrm{kg}^{-1}$ holds under most temperature and pressure conditions. Thus inequality $Lq_s \cdot (q/q_s)^k/(c_{pm}T) \ll 1$ always holds. The right-hand term of (12) can be approximately expressed as $-\delta(Lq_s \cdot (q/q_s)^k)/T$. The approximation can also be verified from the derivation of the GPT's conservation. Hence the following inequality always holds in real atmosphere:

$$q_s \cdot \left(\frac{q}{q_s}\right)^k < q_s. \tag{13}$$

So the assumption for introducing EPT is the sufficient conditions for inducing GPT.

Moreover, ignoring the individual change of c_{pm}, (12) can be transformed into

$$\delta\left(c_{pm}\ln T - R_v \ln p + \frac{L(q_s \cdot (q/q_s)^k)}{T}\right) = 0. \tag{14}$$

Integrating (14), taking exponential operation with the help of $\kappa = R_v/c_{pm}$, the following equation is obtained:

$$\theta^*(T, p) \equiv T\left(\frac{p_0}{p}\right)^\kappa \exp\left(\frac{Lq_s \cdot (q/q_s)^k}{c_{pm}T}\right) = \text{const}, \tag{15}$$

which is conservative. Equation (15) can further be transformed into

$$\theta^*(T, p) = \theta(T, p)\exp\left(\frac{Lq_s \cdot (q/q_s)^k}{c_{pm}T}\right). \tag{16}$$

Similar to the deriving approach of the equation of PT, it is easy to obtain the one for moist atmosphere:

$$c_{pm}\frac{T}{\theta^*}\frac{d\theta^*}{dt} = Q_d. \tag{17}$$

From (17), a conclusion can be drawn that GPT is also conserved in the moist adiabatic process. It should be pointed out that all assumptions in deriving the GPT's conservation are necessary conditions for EPT's conservation. From this point of view, in addition to its conservation, GPT can manifest more accurately the variation of humidity for the real moist atmosphere than EPT.

3. The Comparison of the Distribution for EPT and GPT in Heavy Rainstorm

Recently Gao et al. [22] derived the generalized potential vorticity (GPV) with GPT and diagnosed heat wave weathers during the summer seasons in Beijing. However they have not yet further applied them to analyze torrential rain events. In this paper, we intend to diagnose GPT's distribution within various heavy rain storms and show that GPT has evident advantages over EPT.

3.1. The Distribution of EPT and GPT in Yangtze River and Huaihe River Basin Torrential Rains. The Meiyu is a typical weather phenomenon along the Yangtze River and Huaihe River basins during the early summer season. The comparison of the distribution for EPT and GPT will be made within these Meiyu frontal rainstorms. In late June and middle July, 2003, strong rainstorm and flood disaster occurred in Yangtze River and Huaihe River basins. The onset of Meiyu was on 21st June and the outset on 22nd July. The precipitation mainly occurred during two periods, one from 21st to 28th June when the rainfall was almost concentrated in the Yangtze River basin with a center at the middle Yangtze River, and the other lasting from 29th June to 11th July when the extensive rainbelt was located at Huaihe River basin. Detailed surface precipitation observations can be found in Zhou et al. [27]. We focus on the second period here.

Figure 1 shows the distributions of averaged EPT and GPT at 850 hPa from 29 June to 11 July 2003. Over mainland China, PT is generally smooth and shows weak spatial gradient (Figure omitted). As PT does not include the vapor term, the expected band of vapor gradient associated with the Meiyu front cannot be seen. From Figure 1(a), a large gradient zone of EPT elongates from 30° to 33°N, apparently indicating the feature of vapor gradient across the Meiyu front. But the region of high humidity, due to the moisture transportation by the southwest monsoon, is located in the south side of Meiyu front. In Figure 1(b), the high-value regions of GPT and its strong gradient are located to the south of 33°N from Japan to the Bay of Bengal, which results from the inclusion of specific humidity. No matter how much vapor the atmosphere contains, the content of moisture is surly to be imaged with GPT. So GPT tends to show advantages over EPT.

Seen from the meridional cross-section (Figure 2), the distinct gradient of EPT (Figure 2(a)) lies in the region north of 33°N, which is the confluence zone of the warm and moist air from southwest as well as the dry and cold air from the north, forming the famous Meiyu front in early summer in East Asia. Similar to EPT, two narrow dense zones of GPT isopleths with large vapor gradient exist near the position at 30°N and 33°N, respectively, but the gradient is much larger than that of EPT, which implies plentiful water vapor content concentrated between these two large moist gradient zones. According to the RH isopleths (the dashed lines in Figure 2(b)), the large value zones of GPT gradient coincide well with the regions of RH up to 80%, and GPT's gradients coincide with those of RH well than EPT's, indicating that the

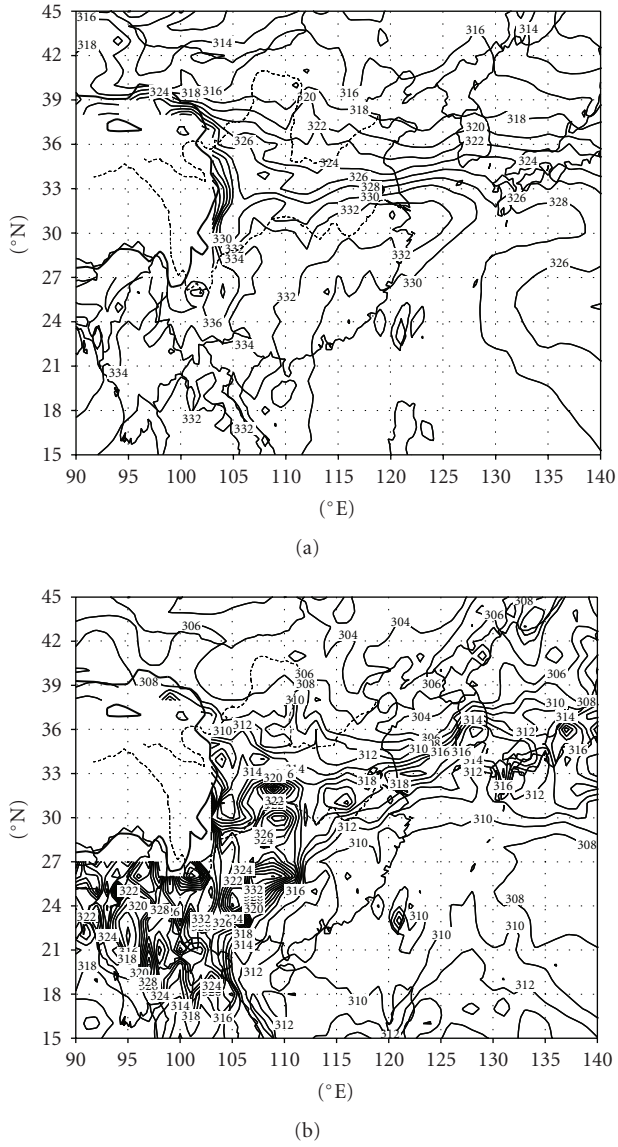

Figure 1: Distributions of the averaged (a) EPT and (b) GPT at 850 hPa from 29th June to 11th July in 2003 (unit in K; isoline interval of EPT and GPT: 2; isoline interval of RH: 10%). The blank zone is the Tibetan Plateau.

expression of GPT involving the moist vapor humidity could reflect the feature of moisture concentration better than EPT during the Meiyu period. Similarities can be found in the Meiyu frontal rainstorms in the Yangtze River basin in 1998 and 1999 as well as the one in the Huaihe River basin in 2007. The observations also indicate that the RH can hardly reach 100%, even in the flooding. So the introduction of GPT for the moist air is capable of describing the distribution of vapor and thermodynamic property of real atmosphere.

3.2. The Distribution of EPT and GPT in the Torrential Rain of North China and in a Typhoon Fung-Wong in 2008. The above cases show the contrast among EPT for saturated moist air and GPT for moist atmosphere during the Meiyu period.

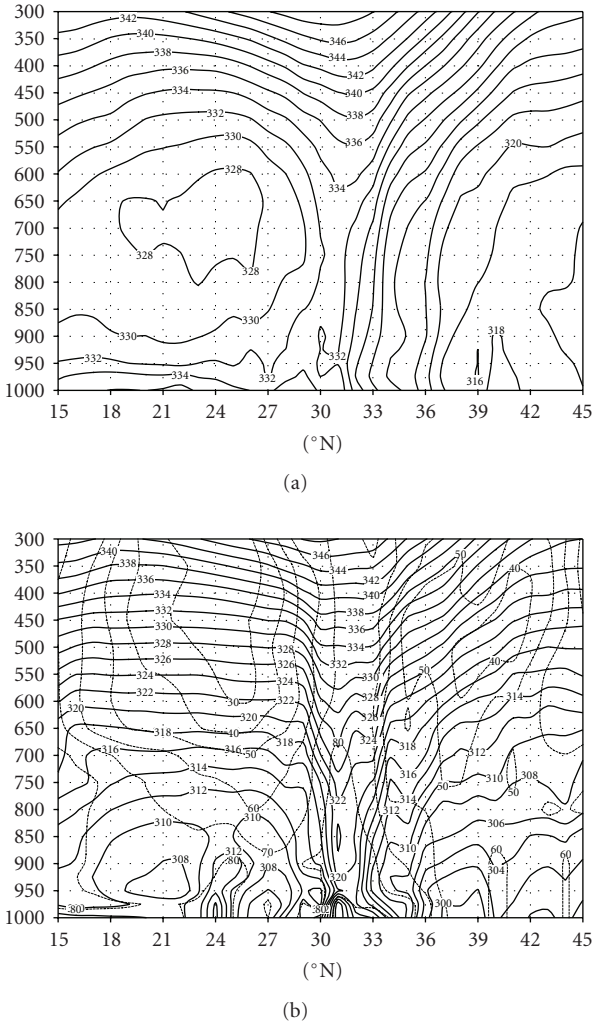

Figure 2: Meridional cross-sections of the averaged (a) EPT and (b) GPT (solid line) and RH (dashed line) along 115°E from 29th June to 11th July in 2003 (unit in K; the intervals: 2, 3, resp.; the interval of RH: 10%).

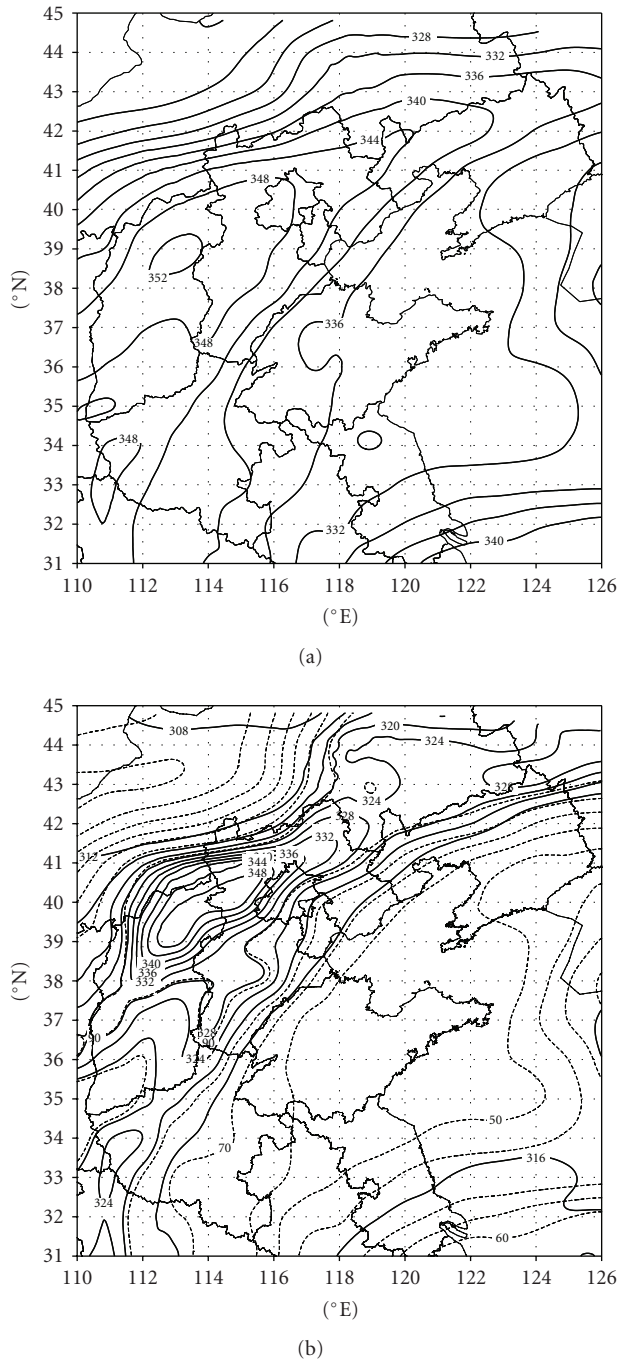

Figure 3: Distributions of (a) EPT and (b) GPT (solid line) and RH (dashed line) at 700 hPa on 12UTC August 2004 (unit in K; the intervals: 4, 4, resp.; the interval of RH: 10%).

China is also often experiencing high-frequent and wide-range torrential rains, so it is necessary to make a comparison with other forms of rainstorms. The heavy rainfall occurring in North China in August 2004 and Typhoon Fung-wong in 2008 is taken as examples. From 11th to 13th August 2004, a heavy rain occurred in North China. Several past studies have simulated and analyzed this event [26]. We thus here only focus on the distributions of these three variables during the event.

An obvious wet trough with the southwest to northeast orientation can also be discerned in Figure 3(a). This trough corresponds to the high-value zone of EPT, indicating that the moisture is transported into the rainfall zone, and the gradient of EPT is accordant with that of RH. For the distribution of GPT, in addition to the coincidence between the two dense gradient zones of GPT (solid line in Figure 3(b)) and RH (dashed line in Figure 3(b)), the southwest-northeast moist trough is also apparent. The center of large values of GPT occurred with RH higher than 90%, which is much clearer than that of EPT. The more significant center and gradients in both sides of the rainbelt for GPT suggest the existence of high moisture concentration.

From the meridional cross sections, similar to Figure 3, a wedge shaped the distribution of EPT from the upper to middle levels, a sign of abundant latent heat release through

the whole atmospheric layer (Figure 4(a)). Obviously, to the north of 38°N (the south side of the strong rainfall region), the EPT values in the mid-lower levels are higher than those north of 42°N, and the EPT gradient in the north and south rainfall zones coincides with the zone of moisture gradient (dashed lines in Figure 4(b)). For the GPT, its isolines extend from the upper to lower air in the heavy rain zones, indicating plentiful water vapor above the rain region. Furthermore, the high-value GPT center overlaps with the high RH center, which is up to 90%. And the large value center of GPT is much narrower than that of EPT. Comparing Figure 4(a) with Figure 4(b), the EPT above the heavy rainfall zones (34∼37°N) does not reveal a dry region with RH lower than 20%. The EPT isolines stretch northward and downward, while the GPT isolines stretch downward in the south of the dry regions and then northward, finally forming a small ridge extending to the downside and a weak trough of GPT occurring in the region that RH is smaller than 20%. The spatial distribution of GPT is much closer to the distribution of water vapor than EPT.

The above analysis is on a heavy rainfall event occurring in North China. In the following, the features of Typhoon Fung-wong with plenty of water vapor are discussed in detail. As the first strong typhoon landed in China in 2008, Fung-wong is special for its large size, large-range influence, and high water vapor content. Particularly it had an imbalanced shape with clouds primarily seen in the south of the center during its early stage. The thick clouds were always located at its southeastern quadrant, accompanied by plenty of water vapor supply, inducing torrential rain with high intensity, large scopes, and long-time influence.

At 14UTC on July 25th, 2008, formed over the east ocean of Philippines, Fung-wong moved westward. Subsequently, it evolved into a severe tropical storm at 08UTC on 26th and into a typhoon at 20UTC on 27th. After landing over the Hualian area of Taiwan at 0630UTC 26th, Fung-wong continued to move northwestward. At 22UTC 28th, it landed at the town of Donghan in Fuqing city of Fujian Province again with the central pressure of 975 hPa and the central maximum wind speed of nearly 33 m s^{-1} (12-grade), and then moved northwestward but decreased gradually. In the afternoon of 30th, it weakened into a tropical storm depression in the northwest of Jiangxi Province with its center shifting southwestward slowly and passing through the southeast of Anhui Province. Fung-wong caused heavy precipitation and flooding in the southeastern coastal region of southern China as well as Jiangxi Province. From the isobaric chart at 850 hPa at 00UTC 28th July, the wind field of Fung-wong (the center located around 23°N, 121°E) had an asymmetrical structure (Figure 5(a)), and the high wind zones, surrounded by abundant water vapor, were situated in its south, east, and north parts. At the same time the RH over the west Pacific Ocean is up to 90%. Moreover, the high-value region of RH within Fung-wong reached 100%. This asymmetrical structure cannot be seen in PT because PT had a relatively smooth structure (Figure 5(b)). As to the EPT (Figure 5(c)), the thermodynamic asymmetrical structure of Fung-wong circulation is evident. The southeastern part of Fung-wong corresponds to the high-value zones of EPT

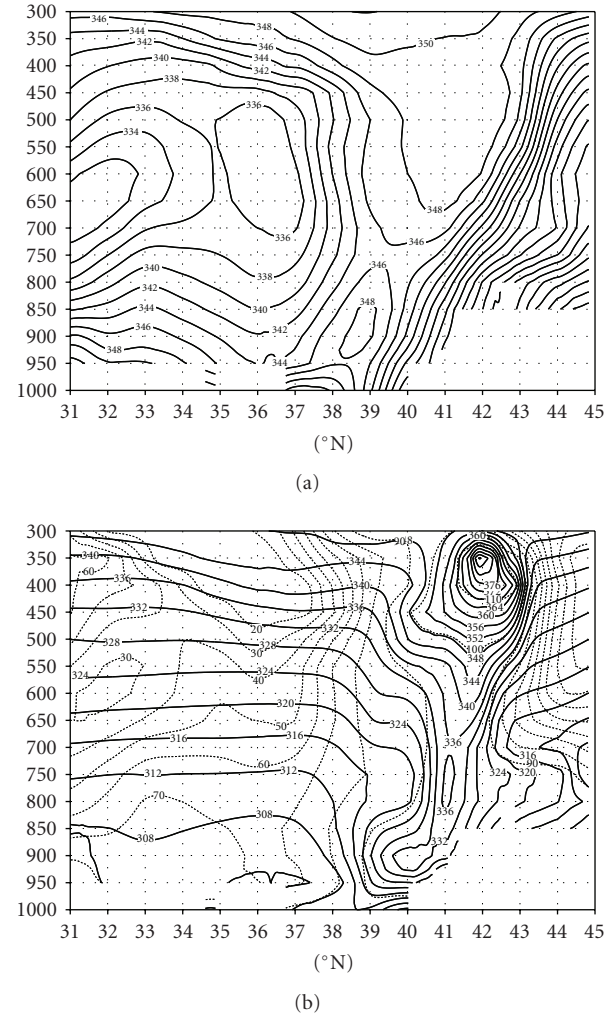

Figure 4: Meridional cross-sections of (a) EPT and (b) GPT (solid line) and RH (dashed line) along 117°E at 12UTC 12th August 2004 (unit in K; the intervals: 2, 4, resp.; the interval of RH: 10%).

(reflecting the high-humidity center), which is also the high-value areas of the EPT gradient, while the central region of Fung-wong is relatively dry. Figure 5(d) shows much denser isopleths for GPT reaching its maximum and high gradient in the region of RH up to 90%, which indicates that the gradient of GPT is larger than that of EPT. Considering that the thermodynamic circulation reveals the most clearest in the GPT distribution and the GPT's high-value zones overlap the region of RH up to 90%, the conclusion can be drawn that GPT not only is able to reflect the thermodynamic structure but also has advantage over PT and EPT in showing the distribution of water vapor fields.

The meridional cross-section (Figure 6) further indicates that water vapor around the eyewall is plentiful from lower levels up to higher levels, with RH reaching above 90% from sea surface to above 350 hPa (dashed line in Figure 6(b)). However, RH near the central of the typhoon is smaller than that of eyewall, about 80%, which shows that water vapor content is convergent around the eyewall

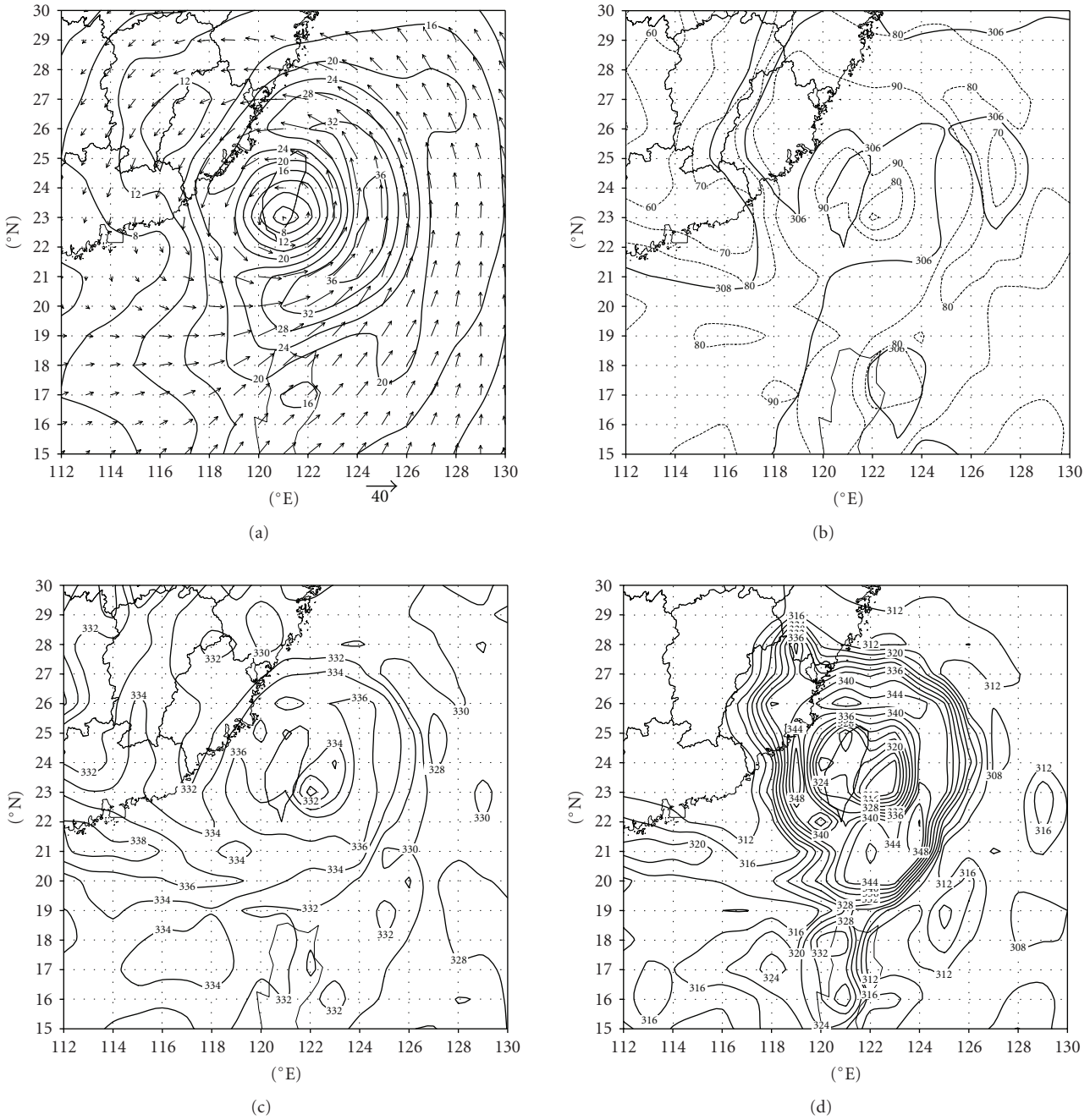

Figure 5: Distributions of (a) wind field (solid: velocity, arrows: wind vector, unit in m s^{-1}), (b) PT (solid line) and RH (dashed line), (c) EPT, and (d) GPT at 850 hPa at 00UTC 28th July in 2008 (unit in K; the intervals: 2, 2, 4, resp.; the interval of RH: 10%).

but it is relatively dry in eyewall, consisting with a general distribution of moisture for typhoon. Since EPT includes the water vapor term, the isopleths around the eyewall of the typhoon form a steep shape, the convective instability zones stretch up to 650 hPa, and EPT has a V-shape pattern from higher levels downward to 800 hPa near the center of typhoon (Figure 6(a)). Compared to the steep GPT isolines (Figure 6(b)), the instability regions is as clear as the EPT's, but the gradient for EPT is not so large as the GPT's. Moreover, accompanying the two gradients bands for GPT, the maximum zone overlaps with the highest water vapor values of the typhoon eyewall at 900 hPa levels. The gradient belt for GPT is more obvious than EPT's at the regions that RH is over 90%, that is, the two regions from 17~20°N and 25~27°N in Figure 6(b).

From the heavy Meiyu front rainfall of Yangtze River and Huaihe River basin to North China rainstorm and to the typhoon Fung-wong, the comparisons of the EPT and GPT distributions indicate that the GPT is able to reflect the effects of moisture and water vapor gradient better than EPT.

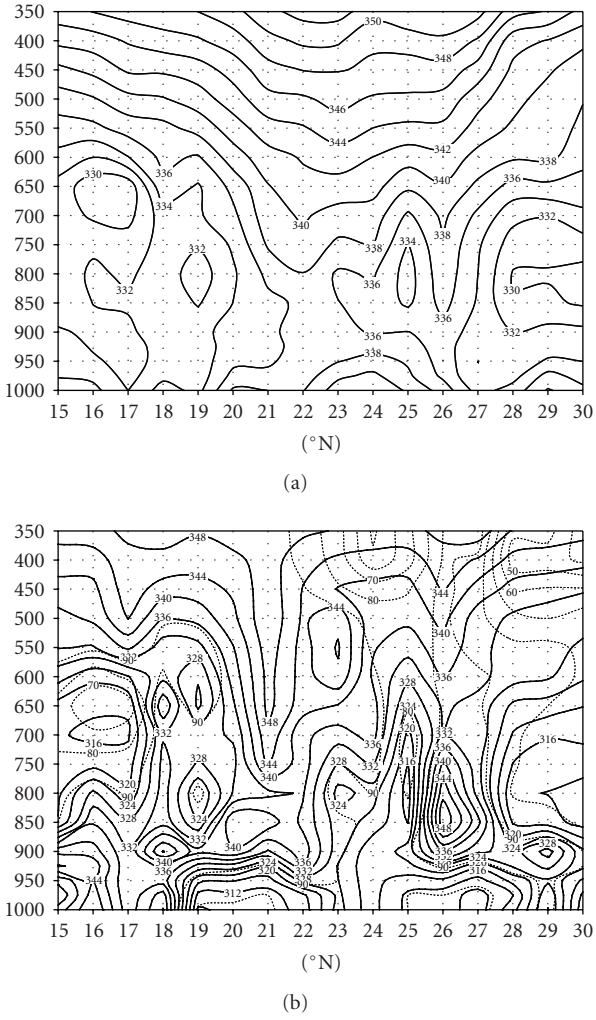

Figure 6: Distribution of (a) EPT and (b) GPT (solid line) and RH (dashed line) along 121°E at 00UTC 28th July 2008 (unit in K; the intervals: 2, 4, resp.; the interval of RH: 10%).

4. Conclusion

A further exploration of the properties and application of the GPT introduced by Gao et al. [7] is carried out in this paper. The physical significance of the condensation probability function invoked in the definition of GPT is discussed, including the derivation of the conservation property of GPT for the nonuniformly saturated atmosphere, tending to enhance GPT's theoretical basis for the moist atmosphere. In the real atmosphere, the air changes from dry state to moist and then to saturated. The introduction of GPT can exactly describe this process. Furthermore GPT can conveniently be applied in the operational analyses of synoptic system. The different distributions among EPT and GPT are compared and analyzed during the periods of Mei-yu heavy rainfall, North China rainfall, and typhoon Fung-wong. The diagnosis results show that GPT, compared with EPT, can manifest the effects of moist concentration and moist gradient more efficiently in heavy rain events. Meanwhile, similar to the EPT in saturated air, GPT is conserved in the moist atmosphere. So like EPT, it can be widely used in studying the dynamic and thermodynamic properties of moist atmosphere in the future.

Acknowledgments

This paper is supported by the State Key Development Program for Basic Research of China (Grant no. 2009CB421505), the Meteorological Special Project of The Ministry of Sciences and Technology of the People's Republic of China (Grant no. GYHY200706020), and the Project of the Natural Science Foundation of China (Grant nos. 40775031 and 40620120437).

References

[1] H. Ertel, "Ein neuer hydrodynamischer Erhaltungssatz," *Naturwissenschaften*, vol. 30, no. 36, pp. 543–544, 1942.

[2] W. A. Robinson, "On the structure of potential vorticity in baroclinic instability," *Tellus, Series A*, vol. 41, no. 4, pp. 275–284, 1989.

[3] Z. H. Cao and H.-R. Cho, "Generation of moist potential vorticity in extratropical cyclones," *Journal of the Atmospheric Sciences*, vol. 52, no. 18, pp. 3263–3281, 1995.

[4] R. F. A. Hertenstein and W. H. Schubert, "Potential vorticity anomalies associated with squall lines," *Monthly Weather Review*, vol. 119, no. 7, pp. 1663–1672, 1991.

[5] S. Gao, T. Lei, and Y. Zhou, "Moist potential vorticity anomaly with heat and mass forcings in torrential rain systems," *Chinese Physics Letters*, vol. 19, no. 6, pp. 878–880, 2002.

[6] S. Gao, T. Lei, Y. Zhou, and M. Dong, "Diagnostic analysis of moist potential vorticity anomaly in torrential rain systems," *Jounnal of Applied Meteorological Science*, vol. 13, no. 6, pp. 662–680, 2002 (Chinese).

[7] S. Gao, X. Wang, and Y. Zhou, "Generation of generalized moist potential vorticity in a frictionless and moist adiabatic flow," *Geophysical Research Letters*, vol. 31, no. 12, Article ID L12113, 4 pages, 2004.

[8] Y. B. Xie, *Synoptic Problems in Moist Baroclinic Atmosphere. Thesis Collection on Torrential Rain*, Jilin Press, Changchun, China, 1978.

[9] L. M. Wang and H. B. Luo, "The basic equations and main characteristics of saturated moist dynamics," *Acta Meteorological Sinica*, vol. 38, no. 1, pp. 44–50, 1980 (Chinese).

[10] G. X. Wu, Y. P. Cai, and X. J. Tang, "Moist potential vorticity and up-slide vorticity development," *Acta Meteorological Sinica*, vol. 53, no. 4, pp. 387–405, 1995 (Chinese).

[11] X. R. Wang, C. E. Shi, and Z. X. Wang, "Non-hydrostatic vertical coordination transition and moist dynamic equations," *Scientific Atmospheric Sinica*, vol. 21, no. 5, pp. 557–563, 1997 (Chinese).

[12] G. J. Tripoli and W. R. Cotton, "The use of ice-liquid water potential temperature as a thermodynamic variable in deep atmospheric models," *Monthly Weather Review*, vol. 109, no. 5, pp. 1094–1102, 1981.

[13] Y. Pointin, "Wet equivalent potential temperature and enthalpy as prognostic variables in cloud modeling," *Journal of the Atmospheric Sciences*, vol. 41, no. 4, pp. 651–660, 1984.

[14] T. Hauf and H. Höller, "Entropy and potential temperature," *Journal of the Atmospheric Sciences*, vol. 44, no. 20, pp. 2887–2901, 1987.

[15] K. V. Ooyama, "A thermodynamic foundation for modeling the moist atmosphere," *Journal of the Atmospheric Sciences*, vol. 47, no. 21, pp. 2580–2593, 1990.

[16] K. V. Ooyama, "A dynamic and thermodynamic foundation for modeling the moist atmosphere with parameterized microphysics," *Journal of the Atmospheric Sciences*, vol. 58, no. 15, pp. 2073–2102, 2000.

[17] L. J. Rivas Soriano and E. L. García Díez, "Effect of ice on the generation of a generalized potential vorticity," *Journal of the Atmospheric Sciences*, vol. 54, no. 10, pp. 1385–1387, 1997.

[18] W. H. Schubert, S. A. Hausman, M. Garcia, K. V. Ooyama, and H.-C. Kuo, "Potential vorticity in a moist atmosphere," *Journal of the Atmospheric Sciences*, vol. 58, no. 21, pp. 3148–3157, 2001.

[19] P. R. Bannon, "Theoretical foundations for models of moist convection," *Journal of the Atmospheric Sciences*, vol. 59, no. 12, pp. 1967–1982, 2002.

[20] A. K. Betts, "Non-precipitating cumulus convection and its parameterization," *The Quarterly Journal of the Royal Meteorological Society*, vol. 99, no. 419, pp. 178–196, 1973.

[21] P. O. G. Persson, "Simulations of the potential vorticity structure and budget of FRONTS 87 IOP8," *The Quarterly Journal of the Royal Meteorological Society*, vol. 121, no. 525, pp. 1041–1081, 1995.

[22] S. Gao, Y. Zhou, T. Lei, and J. Sun, "Analyses of hot and humid weather in Beijing city in summer and its dynamical identification," *Science in China, Series D*, vol. 48, supplement 2, pp. 128–137, 2005.

[23] S. Yang, S. Gao, and D. Wang, "Diagnostic analyses of the ageostrophic $\vec{Q}$ vector in the non-uniformly saturated, frictionless, and moist adiabatic flow," *Journal of Geophysical Research D*, vol. 112, no. 9, Article ID D09114, 4 pages, 2007.

[24] M.-Y. Huang, Y.-H. Xu, and X. Zhou, *Cloud and Precipitation Physics*, Science Press, Beijing, China, 1999.

[25] D. G. Andrews, *An Introduction to Atmospheric Physics*, Cambridge University Press, Cambridge, UK, 2000.

[26] Y. Zhao and S. Gao, "Diagnostic analyses study of convective vorticity vector in torrential rain systems," *Chinese Journal of Atmospheric Sciences*, vol. 32, no. 3, pp. 444–456, 2008 (Chinese).

[27] Y. Zhou, S. Gao, and G. Deng, "A diagnostic study of water vapor transport and budget during heavy precipitation over the Changjiang River and the Huanhe River Basins in 2003," *Chinese Journal of Atmospheric Sciences*, vol. 29, pp. 195–204, 2005 (Chinese).